# ASTR-3415: Astrophysics Course Lecture Notes Section III

Dr. Donald G. Luttermoser East Tennessee State University

> Spring 2003 Version 1.2

${f Abstract}$		
These class notes are designed for use of the instructor and students of the course ASTR-3415: Astrophysics. This is the Version 1.2 edition of these notes.		

# III. The Solar and Stellar Atmospheres

#### A. The Solar Photosphere

- 1. Light sphere  $\equiv$  solar disk, the region of the solar atmosphere where the Sun's white light (i.e., visual continuum) originates. It is a mere 700 km thick! Table III-1 displays some solar facts which you will need throughout the course.
- 2. The solar photosphere is close (although not exactly) to being in hydrostatic equilibrium (HSE) and radiative equilibrium (RE).
  - a) HSE in a plane-parallel atmosphere obeys the relation:

$$\frac{dP}{dz} = -g\rho,\tag{III-1}$$

where P is the total pressure, z represents atmospheric depth, g is the surface gravity, and  $\rho$  is the gas density of a given depth.

**b)** RE follows the relation:

$$\vec{\nabla} \cdot \vec{F}_R = 0, \tag{III-2}$$

where  $F_R$  is the radiative flux.

c) Deep in the photosphere, the energy flux from convection cells  $(F_C)$  must be included in the RE equation:

$$\vec{\nabla} \cdot (\vec{F}_R + \vec{F}_C) = 0. \tag{III-3}$$

3. The Sun, being a stable G2 V star, has a (more or less) constant luminosity. The solar flux at 1 AU is called the **solar constant** and is equal to  $1.3533 \times 10^6 \text{ erg cm}^{-2} \text{ sec}^{-1}$ .

Figure III–1: An intensity contour map of a solar active region made with the Solar Vacuum Telescope on Kitt Peak, Arizona.

- 4. Sunspots are seen in the photosphere (see Figure III-1) that follow an approximate 22-year magnetic cycle (and an 11-year activity cycle).
  - a) The sunspot  $\vec{B}$  field strength is  $\sim 1000$  Gauss  $(\langle \vec{B}_{phot} \rangle \sim 1$  Gauss).
  - b) The ACRIM bolometer aboard the Solar Maximum Mission (SMM) spacecraft detected variations ( $\sim 0.2\%$ ) in the solar irradiance (*i.e.*, solar constant) as displayed in Figure III-2.
  - c) Sunspot groups are called **active regions**. Small bright areas called **facula** are also seen in these regions.
- 5. The photospheric temperature increases with depth (as would be expected from RE). This photospheric temperature profile can be deduced from **limb darkening**.

Figure III-2: SMM/ACRIM observations of the solar irradiance. The large dips correspond to large sunspots crossing the disk.

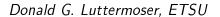
Table III–1: Solar Data

Item	Symbol	Value
Radius	$R_{\odot}$	$6.96 \times 10^{10} \text{ cm}$
Mass	$M_{\odot}$	$1.99 \times 10^{33} \text{ gm}$
Surface Gravity	$g_{\odot}$	$2.74 \times 10^4 \text{ cm sec}^{-2}$
Equatorial Rotation Velocity	$v_{\mathrm{eq}}(\odot)$	$2.0 \times 10^5 \text{ cm sec}^{-1}$
Luminosity	$L_{\odot}$	$3.83 \times 10^{33} \text{ erg sec}^{-1}$
Effective Temperature	$T_{\mathrm{eff}}(\odot)$	5785 K
Angular Size	$lpha_{\odot}$	1919.26" $(1$ " = $725  km)$

- a) Limb darkening is the characteristic of disk center being brighter than the limb of the disk as shown in the intensity contour falloff near the limb in Figure III-3.
- b) The opacity of the solar photosphere allows us to see ~ 700 km into the Sun. As such, we see deeper, hotter layer at disk center, while observations at the limb only "skim" the higher, cooler layers.
- 6. The photosphere begins at the top of the interior convection zone. The tops of the convection cells are seen as **granules** in white light images of the disk. 3-D hydrodynamic models of solar granules can be found in the 26 March 1992 issue of *Nature* under the authorship of Richard Muller.

## B. The Solar Chromosphere

- 1. When the bright photosphere is blocked by the Moon during a solar eclipse, a *red* ring appears around the Moon. This red ring has been coined the **chromosphere** (*color sphere*).
- 2. It has been shown through semi-empirical modeling (i.e., temperature structures derived from a synthetic/observed spectra comparison) that the chromosphere is at a temperature greater than  $T_{\text{eff}}$  (i.e.,  $\langle T_{\text{chromo}} \rangle > \langle T_{\text{photo}} \rangle$ ).
- 3. The most used chromospheric model of the Sun is that of Vernazza, Avrett, and Loeser (VAL) (1973, Astrophys. Journ., 184, 605; 1976 [VAL-I], Astrophys. Journ. Suppl., 30, 1 [VAL-II]; 1981, Astrophys. Journ. Suppl., 45, 635 [VAL-III]).
  - a) In the models presented in these papers, Model C of VAL-III produced synthetic spectra that best reproduced the solar spectrum in the near-UV, optical, IR, and mi-



III-5

Figure III—3: An intensity contour map of the solar disk made with the Kitt Peak Vacuum Telescope. The top image shows the full disk and the lower image shows a magnified image of the limb. Note how the contours rapidly fall off as the limb is approached.

- crowave spectral regions for non-active regions (*i.e.*, the so-called *quiet* regions outside of magnetically active regions sunspots and faculae).
- b) Figure III-4 displays this VAL-III chromospheric model, T(h), and shows the depth of formation for various spectral features (lines and continua).
- c) You need to remember that spectroheliograms of chromospheric lines (i.e., Ca II H & K) show the solar chromosphere to be inhomogeneous  $\Longrightarrow$  chromospheric network.
- d) h = 0 in Figure III-4 represents the depth where the optical continuum originates. Whereas the photosphere is  $\sim 700$  km thick, the chromosphere is  $\sim 2000$  km thick.
- e) The region at h = 500 km, where the chromosphere connects to the photosphere, is called the **temperature** minimum region. This region was once called the reversing layer prior to  $\sim 1970$ .
- f) The  $K_1$ ,  $K_2$ , and  $K_3$  features for Ca II (and similarly, the  $k_1$ ,  $k_2$ , and  $k_3$  features for Mg II) labeled in Figure III-4 were defined in Figure II-1. As can be seen, the  $K_2$  (and  $k_2$ ) feature is formed in the lower/middle chromosphere, and as such, makes this feature very useful in determining chromospheric activity of a star.
- g) The H $\alpha$  core is also formed in the chromosphere. Emission from this line ( $\lambda 6563$ ) is what gives the chromosphere its red color during an eclipse.

Figure III–4: The VAL temperature profile (Model C of VAL-III) for the chromosphere of the Sun. Arrows indicate depths of formation of various spectral features.

- 4. The upper layers in the models of VAL has been superseded by newer models calculated by Fontenla, Avrett, and Loeser (FAL) (i.e., FAL 1990, Astrophys. Journal, 355, 700 [FAL-I]; FAL 1991, Astrophys. Journal, 377, 712 [FAL-II]; FAL 1993, Astrophys. Journal, 406, 319 [FAL-III]; FAL 2002, Astrophys. Journal, 572, 636 [FAL-IV]).
  - a) The FAL models concentrate on the transition region and upper chromosphere.
  - b) These models were generated for the following reasons:
    - i) The VAL models were unable to reproduce the Ly- $\alpha$ , He I, and He II resonance line profiles.
    - ii) The synthetic spectrum of the VAL models also did not correspond with EUV (*i.e.*, extreme ultraviolet) observations of the Sun taken after the VAL models were published.

- iii) Improved and additional physics has been added to the PANDORA radiative transfer code since the VAL models were produced such as:
  - Addition of ambipolar diffusion  $\Longrightarrow$  hydrogen (and helium) atoms diffuse differently in the solar atmosphere as compared to protons and electrons (which are influenced by electric currents). Here diffusion describes how gas "settles" in a potential field it is important to the pressure caused by various species in the gas (i.e., partial pressure) which results from various forces that are present in the gas (i.e., gravity, electric and magnetic fields). Hence neutral atoms diffuse differently than charged particles.
  - Inclusion of an energy balance equation including thermal conduction and input mechanical heating functions.
  - Improvement in partial redistribution (PRD) calculations.
  - Improvement in continuum and bound-bound cross sections.
- c) Figure III-5 (taken from Fontenla et al. 1999, Astrophys. Journal, 518, 480) shows the temperature structure of some of the FAL models. The upper figure shows a blow up of the photosphere and chromosphere and the lower figure shows the transition region and corona. Model 'S' corresponds to a sunspot umbra, 'P' to a bright plage, and 'A' to a faint supergranule cell interior (see below).



Figure III-6: The violet region of the Sun's spectrum. The Ca II  $H_2$  and  $K_2$  chromospheric features are marked.

- d) One should note that the temperature plateau in the upper chromosphere of the VAL-III model seen in Figure III-4 (between 2100 km < h < 2300 km) has disappeared in all of the FAL models. This results from the change to the hydrogen ionization equilibrium (hence the hydrogen ion to neutral ratio) from the inclusion of ambipolar diffusion in the pressure calculations  $\Longrightarrow$  Ly- $\alpha$  can now be fitted accurately without this temperature plateau!
- 5. Figure III-6 shows a sample of the solar spectrum in the violet (3825 Å 4190 Å). The Ca II H (3968 Å) and K (3934 Å) lines are the two strongest lines in the visual solar spectrum. The chromospheric  $H_2$  and  $K_2$  features can be seen near the cores of these lines. As can be seen, they are quite weak  $\Longrightarrow$  the Sun is a chromospherically *inactive* star.
- **6.** The activity of the Sun varies ( $\sim$ 11 years in terms of sunspot

Figure III–7: A comparison of the Ca II chromospheric emission feature from an active region (i.e., plague) and from the "quite" Sun.

numbers and  $\sim 22$  years in terms of the magnetic cycle) and during sunspot maximum (i.e., active Sun), the  $K_2$  and  $H_2$  emission get stronger (see Figure III-7). Active regions in chromospheric light, display large bright patches called **plagues** (analogous to faculae in the photosphere, although larger in size).

- 7. Supergranules can be seen in "chromospheric light" (i.e.,  $H\alpha$ ), which are a collection of many granules. They are associated with the solar magnetic field (see Figure III-8).
  - a) Spicules (flame-like structures) are seen on the boundaries of the supergranules.
  - b) Spicules are at chromospheric temperatures that rise from the chromosphere to a height of 9000 km at an average velocity of  $25 \text{ km s}^{-1}$ .
  - c) They are  $\sim 900$  km wide and last from 5 to 10 minutes.

Figure III–8: Schematic of the solar spicule structure.

d) Figure III-8 shows a schematic of the spicule structure and their association with supergranules.

#### C. The Solar Corona

- 1. Figure III-9 shows the most up to date representative models of the solar corona. Meanwhile, Figure III-9 shows the temperature structure of the average Sun, based on the VAL models, from the base of the photosphere to the lower corona.
  - a) The **corona** is the hottest of the 3 layers in the solar atmosphere  $(T \sim 1 2 \times 10^6 \text{ K})$ , however the particle density is very low compared to the photosphere so that the energy density in this layer is very low.
  - b) The corona extends out to  $\sim 2R_{\odot}$ , however its size changes over the solar activity cycle. It is inhomogeneous, structured via solar coronal loops and coronal holes.
  - c) The region between the chromosphere and corona is very

Figure III-9: The VAL temperature profile of the complete solar (average) atmosphere.

thin ( $\sim 500$  km) and has a very large temperature gradient ( $dT/dh \sim 1000$  K/km). This region is called the **transition region** (50,000 K < T < 500,000 K). C IV at 1550 Å is a transition region spectral indicator for stars.

- 2. The corona (i.e., crown) was discovered in ancient times during solar eclipses although its nature wasn't appreciated until the mid-1900s. The corona seen in white light (during an eclipse or with a coronagraph) is actually composed of 2 components.
  - a) The K-corona is ionized gas and produces a continuum via e<sup>-</sup>-scattering (very bright in X-rays and radio  $\lambda$ s). This ionized gas also produces strong emission lines of highly ionized elements in the EUV and X-ray region.
  - b) The F-corona is caused by interplanetary dust ( $\sim 1 \mu m$  in diameter). Fraunhofer lines are seen from this corona (photospheric light scattered from dust) this corona

is not included as part of the solar atmosphere.

- c) From this point on, the term "corona" will refer to the K-corona.
- 3. The temperature of the "average" corona is essentially constant. Thermal conductivity is very efficient in this region due to the high temperatures. Conduction redistributes the energy throughout the corona and prevents T from falling off rapidly in either direction of  $T_{max}$ .
- 4. There are essentially 3 types of coronal structure.
  - a) Active regions:
    - i) Loop structures (closed B-fields, 10<sup>3</sup> 10<sup>4</sup> km in diameter) that are bright over the entire spectrum
       — brightest at X-ray λs.
    - ii) Overlie sunspots but can persist long after a sunspot disappears prominent when the Sun is active.
  - b) Quiet corona:
    - i) Loops that are somewhat larger and cooler than active region loops.
    - ii) Most of the "corona" is in this phase.
  - c) Coronal holes:
    - i) Large regions of cooler gas seen at the solar poles and at mid-latitudes when the Sun is active.
    - ii) No loops seen in these regions  $\Longrightarrow$  open B-field.

#### D. Solar Wind

- 1. The solar wind is a low density stream of charged particles emitted from the Sun. It is composed of a high energy (*i.e.*, velocity) component and low energy component. Skylab determined the high energy component originates from the (mid-latitude) coronal holes.
- 2. The solar wind is a thermal wind  $\Longrightarrow$  material that is "boiled" off of the Sun in the hot corona. We will discuss these types of winds in more detail toward the end of the course.
- 3. The Sun loses  $10^{-14} M_{\odot}/\text{yr}$  via the solar wind  $\Longrightarrow$  a "little girlyman" in comparison to the  $10^{-6} M_{\odot}/\text{yr}$  long period variable stars lose or the  $10^{-3} M_{\odot}/\text{yr}$  some WR stars lose.

#### E. Chromospheric and coronal heating

- 1. Much is still unknown about the heating mechanisms of the outer solar atmosphere. As mentioned before, RE dictates that dT/dz > 0 (z is in the opposite sense of  $h \Longrightarrow z$  increases inward, z = const h), what causes dT/dz < 0 above  $T_{\min}$ ?
- 2. The energy equation  $\vec{\nabla} \cdot \vec{F}_{\rm R} = 0$  (we'll ignore convection in these layers) must be rewritten in the form

$$\vec{\nabla} \cdot (\vec{F}_{R} + \vec{F}_{mech}) = 0, \tag{III-4}$$

where  $F_{\text{mech}}$  is a flux term due to some mechanical energy input. This extra mechanical energy can force dT/dz < 0.

**3.** Hydrodynamic (*i.e.*, acoustic) waves play an important role in heating the lower chromosphere. Rising granules give rise to longitudinal compression sound waves which propagate outward

into the low density outer layers. These waves damp out quickly and never make it past the transition region.

- **4.** Magnetohydrodynamic (*i.e.*, Alfvén waves  $\Longrightarrow$  transverse waves in a *B*-field) waves are mainly responsible for heating the corona.
  - a) Coronal activity corresponds to the appearance of photospheric, high *B*-field, active regions.
  - b) The energy from Alfvén waves must be converted to acoustic waves before the gas can be heated.
- **5.** Conduction is another flux term that must be included in the energy equation at coronal temperatures.
  - a) It acts as an energy conduit  $\Longrightarrow$  just moves energy around.
  - b) The upper chromosphere may be heated from energy conducted from the corona through the transition region ⇒ chromospheric activity corresponds to active region appearance as well.

## F. Stellar Photospheres

- 1. As defined by the Sun, <u>all</u> stars have photospheres a region of a stellar atmosphere where the continuum (and many absorption lines) arise. Table III-2 shows the dominant continuous opacity sources for various spectral types.
- 2. Stellar photospheres are generally modeled under the assumption of HSE and RE (as is with the Sun). However, there are some cases where these assumptions are not valid (especially HSE).

Spectral Type	Dominant Continuous Opacities
О	Electron scattering, H b-f
В	H b-f
A	H b-f; H f-f
F	H b-f; H f-f; H <sup>-</sup> b-f; H <sup>-</sup> f-f
G	H <sup>-</sup> b-f; H <sup>-</sup> f-f
K	H <sup>-</sup> b-f; H <sup>-</sup> f-f; Neutral Metals b-f
M, S, N, R	H <sup>-</sup> b-f & f-f; Metals b-f; H, H <sub>2</sub> , He Rayleigh Scattering

Table III–2: Continuous Opacity Sources for the Various Spectral Types

- a) When they are young, very massive stars have very high mass loss due to strong stellar winds ⇒ the Wolf-Rayet stars. HSE is not longer valid.
- b) Certain red giant stars go through stellar pulsations the photospheres move outward then inward (e.g., Cepheids, RR Lyr, & Mira-type variable stars). These pulsations set up large shock waves that propagate outward through the photosphere into outer atmospheric layers ⇒ HSE and RE are not valid in these cases.
- 3. Stellar photospheres are typically modeled under the assumption that the gas is in Local Thermodynamic Equilibrium (LTE).
  - a) In thermodynamic equilibrium (TE) the intensity of radiation does not depend upon spatial position or direction so that the radiation field is homogeneous, isotropic, and described by the kinetic temperature of the particles in the gas in the Planck function  $I_{\nu} = B_{\nu}(T_{\rm kin})$ .
  - b) Often, it is assumed that particle kinetic temperature is equal the the electron temperature, hence  $I_{\nu} = B_{\nu}(T_e) = B_{\nu}(T)$ .

c) Particles in thermal equilibrium, and often when this condition is not met, have velocities that follow the Maxwellian distribution law:

$$f(v) dv = \left(\frac{m}{2\pi kT}\right)^{3/2} \exp\left(-\frac{mv^2}{2kT}\right) 4\pi v^2 dv, \quad \text{(III-5)}$$

where T is the equilibrium temperature.

i) Most probable velocity:

$$v_o = \sqrt{\frac{2kT}{m}}. (III-6)$$

ii) Root-mean-square (rms) velocity:

$$v_{\rm rms} = \sqrt{\frac{3kT}{m}};$$
 (III-7)

and along the line-of-sight (1D):

$$v_{\rm rms}(\ell os) = \sqrt{\frac{kT}{m}}.$$
 (III-8)

iii) Mean velocity:

$$\overline{v} = \sqrt{\frac{8 \, kT}{\pi \, m}}.\tag{III-9}$$

- d) Number densities of levels in the same stage of ionization for particles in TE follow a **Boltzmann distribution** given by Eq. (I-29).
- e) The number density of various stages of ionization for a given species in TE follows the **Saha equation** given by Eq. (I-30). Note that the Saha equation assumes  $e^-$ s ionize the atom/ion.
- f) Stars emit light, hence lose energy. As a result, the atmospheres of stars cannot be in *strict* TE (*i.e.*, a tem-

perature gradient exists). However, if a photon's mean-free-path (mfp) is so small that it doesn't see the gradient, equilibrium conditions are achieved locally, where the local equilibrium temperature is the local electron temperature  $\Longrightarrow$  local thermodynamic equilibrium or (LTE).

- g) When LTE is valid, number densities are designated with an \*-superscript  $\rightarrow n_i^*$ .
- h) If a photon's mfp is large enough that the atmospheric temperature gradient is *seen*, number densities can be derived by assuming all transition rates <u>balance</u> each other  $\Longrightarrow$  statistical equilibrium (SE), also called non-LTE (NLTE).
  - i) Radiative rates which are derived from the mean intensity of the gas and the transition's oscillator strength.
  - ii) Collisional rates which are derived from the electron density and the transition's cross-section to an electron collision.
- 4. Geometry: One of two assumptions are made concerning the spatial derivatives, both reduce these derivatives to one component  $\implies$  thus the atmosphere must be (and is assumed to be) homogeneous parallel to the surface of the star.
  - a) Plane-parallel atmospheres imply that the thickness of the atmosphere (L) is very small with respect to the radius of the star  $(R_{\star})$ , so that  $\vec{\nabla} \to \frac{d}{dz}$  (or  $\frac{d}{dh}$ ), where z generally increases inward (and h outward). Note that some modelers set z=0 at the top of the atmosphere  $(\tau=0)$  and others set z=0 at  $\tau_{5000}=1$ , where  $\tau_{5000}$  is

the optical depth of the continuous opacity at 5000 Å.

- b) Spherically-symmetric geometries are used when  $L \ge 0.1R_{\star}$ , then  $\vec{\nabla} \to \frac{d}{dr}$ , where r = 0 is at the center of the star and increases outward.
- 5. Hydrostatic Equilibrium (or HSE) results from the assumptions of a static atmosphere in a steady state with negligible stresses and electromagnetic fields. With these assumptions, we can write

$$\frac{dP}{dz} = g\,\rho\tag{III-10}$$

for a plane-parallel atmosphere with z increasing inward. For a spherically-symmetric atmosphere,

$$\frac{dP}{dr} = -\rho \, \frac{GM}{r^2},\tag{III-11}$$

with r increasing outward. The pressure in these 2 equations is the <u>total</u> pressure:

$$P = P_g + P_{\xi} + P_{\text{rad}}. \tag{III-12}$$

a) The microturbulent pressure is given by

$$P_{\xi} = \rho \frac{\xi^2}{2} = P_g \frac{\overline{m}\xi^2}{2kT} = P_g \frac{\mu m_{\rm H}\xi^2}{2kT} ,$$
 (III-13)

where  $\xi$  is the **microturbulent velocity** and  $\mu$  is the **mean molecular weight** ( $\sim 0.6$  for solar compositions and ionizations; note that pure neutral hydrogen has  $\mu = 1$  and pure ionized hydrogen has  $\mu = 0.5$ ) and  $\overline{m}$  is the mean mass of the free particles given by

$$\overline{m} = \sum_{\beta} m_{\beta} N_{\beta} / \sum_{\beta} N_{\beta} ,$$
 (III-14)

where  $\beta$  includes all atomic, ionic, molecular species and electrons.

b) The Equation of State relates the gas pressure  $P_g$  to other thermodynamic variables. Generally the *ideal gas law* is assumed for the equation of state:

$$P_g = NkT = \frac{\rho}{\overline{m}}kT = \frac{\rho kT}{\mu m_{\rm H}} . \qquad (III-15)$$

i) We can rewrite Eq. III-15 in the following form:

$$P_q = [(1 + Y - X_2)N_{\rm H} + n_e]kT, \qquad (\text{III-16})$$

where  $Y = N_{\text{He}}/N_{\text{H}}$  is the helium fraction,  $X_2 = N(\text{H}_2)/N_{\text{H}}$  is the molecular hydrogen fraction, and  $N_{\text{H}}$  is the total hydrogen density.

- ii) Over the last 20 years, work has begun on developing an equation of state for stellar atmospheres (T ≤ 10<sup>7</sup> K and ρ ≤ 10<sup>-2</sup> gm/cm³) based on the method of free energy minimization (Hummer, D.G. and Mihalas, D. 1988, Astrophys. Journ., 331, 794; Mihalas, D., Däppen, W., and Hummer, D.G. 1988, Astrophys. Journ., 331, 815; Däppen, W., Mihalas, D., Hummer, D.G., and Mihalas, B.W. 1988, Astrophys. Journ., 332, 261). We shall not discuss this method here due to its complexities.
- c) The radiation pressure  $P_{\text{rad}}$  is fairly complicated to determine. However, for an isotropic radiation field, the radiation pressure is

$$P_{\rm rad} = \frac{1}{3} a T^4,$$
 (III-17)

where  $a=7.564\times 10^{-15}~{\rm erg/cm^3/K^4}$  is the radiation constant.

**6.** The mass density can be expressed as

$$\rho = m_{\rm H}(1+4Y)N_{\rm H},$$
(III-18)

where  $m_{\rm H}$  is the atomic mass of hydrogen. Here we use 4 for simplicity instead of  $m_{\rm He}/m_{\rm H}=4.0026$  and we ignore  $m_e n_e$  in Equation III-18. The abundances of the other elements are assumed to be too small to contribute to P and  $\rho$ . The electron density can be split into 2 parts so that

$$n_e = (R+Z)N_{\rm H},\tag{III-19}$$

where  $R = n_p/N_{\rm H}$  is the fraction of electrons from hydrogen and  $Z = n_e/N_{\rm H}$  from elements other than hydrogen.  $Z \sim$  the relative abundance of ionized elements (e.g.,  $\sim 10^{-4}$  when  $R \ll 1$ ), but at high temperatures, Z can be  $\sim 0.1$  or 0.2 from single or double ionization of helium. R and Z are calculated separately.

## G. Introduction to Chromospheres and Coronae.

- 1. The Linsky-Haisch or Coronal Dividing Line (CDL): Linsky and Haisch (1979, Astrophys. Journ. (Letters), 229, L27) determined that the cool half of the Hertzsprung-Russell (H-R) diagram is divided into 2 distinct regions: F-M dwarfs and late F through early K giants are characterized by prominent chromospheric ( $T \leq 10^4$  K) and higher temperature ( $2 \times 10^4 2 \times 10^5$  K) emission lines in the far-ultraviolet IUE spectra; single red giants later than about K2 III and supergiants later than about G5 Ib are characterized by generally weaker chromospheric emission and little or no evidence for higher temperature species.
  - a) Essentially, stars on the warm side of the CDL show both Mg II h and k emission and C IV ( $\lambda\lambda$ 1548,1551) emission, whereas stars on the cool side only show Mg II emission (see Figure III-10).

Figure III–10: H-R diagram showing the location of the CDL.

region lying at the base of the corona. They suggested that the apparent lack of C IV in stars implies a lack of a corona, hence the term "coronal dividing line". Subsequently, Ayres et al. (1981, Astrophys. Journ., 250, 293) used the Einstein IPC detector to confirm the reality of the proposed CDL: Stars to the left have measurable Einstein X-ray fluxes, but those to the right do not.

- c) There seems to be a correlation between chromospheric activity and surface convection zones in stars and the thought is that some sort of mechanical heating mechanism, driven from the surface convection zone, is responsible for the departure from radiative equilibrium that generate chromospheres and coronae.
  - i) The following question has been asked: "What is the heating mechanism responsible for the appearance of chromospheres and coronae?"
  - ii) A good theoretical basis is needed to answer this question. The trouble is that there are many possible mechanisms.
  - iii) One method used in isolating the heating mechanism is to construct a semi-empirical chromospheric model: Produce a synthetic spectrum of features formed in the chromospheric depths, compare the synthetic spectrum with observations, and adjust the temperature-density stratification of the chromospheric model until the 2 spectra match.
  - iv) Once one has a temperature distribution that matches observations, one can make thermodynamic calculations with various heating mechanisms to isolate the heating mechanism that produces the requires temperature profile.
  - v) Similar types of analyses have been carried out for the solar corona based upon emission measure analysis (e.g., my undergraduate thesis dealt with this topic).

2. In the modeling of stellar chromospheres and coronae, it is often more convenient to express the radiative equilibrium equation (e.g., Eq. III-2) as a total energy equation:

$$\vec{\nabla} \cdot (\vec{F}_{\rm rad} + \vec{F}_{\rm conv} + \vec{F}_{\rm cond} + \vec{F}_{\rm mech}) = 0$$
 or 
$$\frac{d}{dr} \left( F_{\rm rad} + F_{\rm conv} + F_{\rm cond} + F_{\rm mech} \right) = 0$$
 (III-21)

for one-dimensional geometries.

- a)  $F_{\text{rad}}$  is the **radiative flux** determined from the equation of radiative transfer.
- b)  $F_{\text{conv}}$  is the **convective flux** determined from the theory of convection  $\Longrightarrow$  typically the **mixing-length theory** is used to describe this flux.
- c) At coronal temperatures  $(T > 10^5 \text{ K})$ , the **conductive** flux is an important term in the energy equation:

$$\vec{F}_{\text{cond}} = -\kappa \, \vec{\nabla} T = -\kappa_{\circ} \, T^{5/2} \, \vec{\nabla} T, \qquad (\text{III-22})$$

where  $\kappa$  is called the *conductivity*, and  $\kappa_{\circ} \approx 8 \times 10^{-7} \text{ erg}$  cm<sup>-1</sup> s<sup>-1</sup> K<sup>-7/2</sup>. For a one-dimensional geometry,

$$-\vec{\nabla} \cdot \vec{F}_{\text{cond}} = \frac{d}{dr} \left( \kappa_{\circ} T^{5/2} \frac{dT}{dr} \right). \tag{III-23}$$

- d)  $F_{\text{mech}}$  is the **mechanical energy flux**  $\Longrightarrow$  a nonthermal heating source. It is this term that gives rise to stellar chromospheres and coronae.
- 3. Heating Mechanisms. In recent years it has become clear that the heating phenomena in chromospheres and coronae cannot be explained by a single process, but rather due to the action of a multitude of mechanisms. Some of these may operate globally, others only in particular physical situations.

- a) At the present time it is not possible to decide which mechanisms are the important ones, in spite of considerable effort, as the observationally basis for each proposed process is rather weak and the theoretical development of many mechanisms could only lead to an unfair verdict. We will introduce some of the suspected important mechanisms here, however before we begin, we must define what we mean by chromospheres and coronae.
- b) Typically stellar chromospheres and coronae are assumed to be solar-like in a physical sense. However here, we will use the general term *chromosphere* to indicate dT/dr > 0 and  $T \leq 20,000$  K, which presents itself through emission features of singly-ionized metals, particularly Mg II h and k and Ca II H and K, whether such emission is produced by a solar-type chromosphere or due to large scale phenomena such as global shock waves.
- c) The term corona is used here to indicate dT/dr > 0 and T > 100,000 K, which presents itself through emission features of highly-ionized metals and a substantial X-ray flux.

## 4. Various Mechanical Heating Mechanisms

- a) Acoustic wave heating: A stellar surface convection zone, as is the case for all turbulent flow fields, invariably leads to the generation of a spectrum of acoustics waves.
  - i) The mechanical energy flux  $F_{\text{mech}}$  carried by the upwardly propagating acoustic waves for sufficiently high frequency is given by

$$F_{\rm mech} = \rho \, \overline{v}^2 \, c_s \, , \qquad (\text{III-24})$$

where  $\rho$  is the gas density,  $\overline{v}$  is the average gas

velocity, and  $c_s$  is the sound speed.

ii) The sound speed is determined by

$$c_s = \left(\frac{dP}{d\rho}\right)^{1/2} \approx \left(\frac{\gamma P}{\rho}\right)^{1/2} = \left(\frac{\gamma kT}{\mu m_{\rm H}}\right)^{1/2},$$
(III-25)

where  $\gamma$  is the adiabatic constant given by

$$\gamma = \frac{C_P}{C_V} \,, \tag{III-26}$$

with  $C_P$  and  $C_V$  representing the specific heats ( $\equiv$  the amount of heat to raise the temperature by one degree for a given substance) at constant pressure and constant volume, respectively.

iii) If we let Q equal the total amount of heat energy and U be the internal energy of the gas (both described in far more detail in the thermodynamics course), the specific heats can be determined from

$$C_V = \left(\frac{dQ}{dT}\right)_V = \left(\frac{\partial U}{\partial T}\right)_V$$
 (III-27)

$$C_P = \left(\frac{dQ}{dT}\right)_P = \left(\frac{\partial U}{\partial T}\right)_V + P\left(\frac{\partial V}{\partial T}\right)_P \text{(III-28)}$$

iv) Since the temperature in the photospheric layers does not vary by much, if radiation damping is small, the conservation of wave energy flux requires that

$$v \sim \rho^{-1/2}$$
 . (III-29)

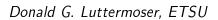
v) The density decrease of the outer atmosphere thus results in a rapid growth of the wave ampli-

tude and, due to the nonlinear terms in the hydrodynamic equations, leads to shock formation, shock dissipation, and heating of the outer stellar layers.

- vi) Acoustic waves are generally separated into two modes: short period (important in main sequence stars) and long period waves (important in pulsating stars: Cepheids, RR Lyrae, and Mira-type variable stars).
- b) Heating by fast and slow magnetoacoustic body waves: In the absence of gravity and for a perfectly conducting, compressible, uniform gas in a homogeneous magnetic field, there exists 3 types of body waves, the Alfvén-mode, fast-mode, and slow-mode waves. The latter 2 wave types are also called magnetoacoustic waves, as these waves show gas pressure fluctuations. Alfvén waves, which will be discussed in the next subsection, do not show gas pressure or density fluctuations.
  - i) About 25 years ago, it was found that the magnetic field at the solar surface is not homogeneous, but appears rather in the form of highly concentrated flux tubes, which are located at the boundaries of the granulation and supergranulation cells.
  - ii) A powerful approach to treat these flux tubes is to assume that the physical quantities do not change much over the tube cross-section and that they are given essentially by their values at the tube axis. For these so-called thin flux tubes, there exists 3 wave modes: the longitudinal or

sausage mode, the transverse or kink mode, and the torsional mode (see Figure III-11).

- iii) The latter 2 wave types to first order do not show fluctuations of the tube cross-section and thus do not have gas pressure variations. These wave thus are similar to the Alfvén waves.
- iv) Propagating magnetic waves in an ionized (or partially ionized) medium will induce motions in the gas and produce acoustic waves hence magnetoacoustic. We will couple these magnetoacoustic waves into the weak shock theory of the previous theory (the weak shock approximation is not bad here since the energy transfer from the magnetic waves to the acoustic waves may not be very efficient).
- c) Alfvén waves: The principle restoring force of Alfvén waves is magnetic tension. Alfvén waves propagate along the magnetic field lines.
  - i) As such, Alfvén wave energy always propagates along the direction of the magnetic field.
  - ii) Alfvén waves are pure sheer waves and to first order are not affected by the compressibility of the medium or by buoyancy forces. The waves never show evanescence or total internal reflections. As such, they are a prime candidate for the primary coronal heating mechanism since they can reach the corona directly from the convection zone.



III-30

Figure III–11: Distortion of a flux tube in the sausage, kink, and torsion modes.

- H. Chromospheric Models. Chromospheric modeling is determined through a semi-empirical approach. Some authors have tried to determine "global" parameters of chromospheres through line ratios and emission measures. We will discuss as few examples of these first and then describe some examples of semi-empirical chromospheric modeling.
  - 1. Empirical techniques have been used to determine information on the mean temperatures and densities of stellar chromospheres. One determines mean chromospheric temperatures by measuring the integrated flux of lines formed in the chromosphere (i.e., Mg II or Ca II).
  - 2. Semi-empirical modeling is a procedure used to determine detailed information on chromospheric structure. A chromospheric temperature rise is attached to a photospheric model representative of a star and this temperature profile is adjusted until synthetic spectra from the model matches the observed spectra. We will investigate 2 examples here of model chromospheres calculated semi-empirically.
    - a) First we re-examine the solar chromosphere as modeled by Vernazza, Avrett, and Loeser (1981, Astrophys. Journ. Suppl., 45, 635), where the temperature structure was shown in Figure III-4. This model was constrained by chromospheric continuum emission in the far-IR and far-UV, the Lyman-α line (though these models did not fit this profile well), Ca II H and K, and Mg II h and k. The greater the number of chromospheric indicators used, the better constrained the model.
    - b) From this model, which represents an averaged chromosphere on the quite Sun, much work has been done to determine the chromospheric heating mechanism for the Sun. To do this heating mechanism analysis, one must

- know the net radiative cooling rates  $(dF_{\rm rad}/dr)$  for important chromospheric opacities.
- c) Some of the first semi-empirical models of stellar chromospheres were done by members of the Cool Star Mafia in Boulder, Colorado under the direction of J.L. Linsky. Ayres, Linsky, and Shine (1974, Astrophys. Journ., 192, 92) developed such a model for Procyon and later Ayres and Linsky (1975, Astrophys. Journ., 200, 660) constructed a semi-empirical chromospheric model for Arcturus based on the Ca II H and K profiles and the Ca II infrared triplet.
- d) Many more models have been done since for these stars and others, typically determined by the more opaque Mg II h and k lines.
- e) From semi-empirical models of the Sun, Procyon, and Arcturus, Ayres and Linsky (1975) noted that the temperature minimum in these stars scaled as  $T_{\rm min}/T_{\rm eff} \approx 0.77$  and that there seemed to be a trend of increasing mass at the temperature minimum with decreasing gravity, which results in explaining the Wilson-Bappu effect (see §I.B.4). For a review of stellar chromosphere modeling prior to 1980, see Linsky (1980, Ann. Rev. Astron. Astrophys., 18, 439).
- I. Coronal Models: Stellar coronal models are generally based upon emission measure analysis from observed X-ray and radio fluxes. Recently, theoretical calculations are being made based on earlier solar work.
  - 1. Skylab discovered that the solar corona is very inhomogeneous with 3 distinct structures:

- a) Active regions which are composed of hot coronal loops  $(T > 3 \times 10^6 \text{ K}).$
- **b)** Quite corona which are composed of cool coronal loops  $(10^6 < T < 3 \times 10^6 \text{ K}).$
- c) Coronal holes with no apparent loop structures.
- 2. The most accurate manner to model these solar coronal loops (or in the stellar case, stellar coronal loops) is to use a full blown magnetohydrodynamic calculation. It is useful to note here that the corona is essentially an optically thin medium, which means that radiative losses can accurately be determined with approximate techniques as such, one doesn't need to do radiative magnetohydrodynamics. The radiative losses are simply accessed via a look-up table based on optically-thin radiative transfer calculations. Such radiative loss functions can be found in Cox and Tucker (1969, Astrophys. Journ., 156, 87) and Raymond, Cox, and Smith (1976, Astrophys. Journ., 204, 290).
- 3. Solar coronal loops have been seen to remain stable for days and even weeks and, during this time, are called *quasi-static* solar coronal loops (see Figure III-12). Models have been made of these quasi-static loops (see e.g., Rosner, Tucker, and Vaiana 1978, Astrophys. Journ., 220, 643; Vesecky, Antiochos, and Underwood 1979, Astrophys. Journ., 233, 987) based on HSE and loop geometry. Such models are then tested by determining the emission measure of the loop ( $\int n_e N_H ds \approx \int N_H^2 ds$ ) and comparing it to the emission measure determined from observations.

Figure III–12: A representative model for a quasi-static solar coronal loop.

4. Rosner, Tucker, and Vaiana (1978) determined a scaling law for loops

$$T_{\text{max}} \approx 1.4 \times 10^3 \, (P \, L)^{1/3} \,,$$
 (III-30)

where  $T_{\text{max}}$  is the maximum temperature of the loop (found at the apex of the loop), P is the average pressure in the loop, and L is the loop length from one footpoint to the other (typically  $\sim 10^5$  km). They also determined that their models were consistent with either Alfvén wave dissipation or coronal current heating for the coronal heating mechanism but inconsistent with acoustic mode damping.

## J. Chromospheric Inhomogeneities

1. When spectroheliograms (full-disk maps of the Sun at one wavelength) are made of the Sun with chromospheric lines, the chromosphere does not look uniform. This observed inhomogeneity is called the **chromospheric network**.

- 2. T.R. Ayres has noted (see 1990, in *Cool Stars, Stellar Systems, and the Sun*, ed. G. Wallerstein, ASP:San Francisco, p.106) that the lines of the CO  $\Delta v = 1$  (v for vibrational transition) bands, which form essentially in LTE and have a rather high opacity in the solar chromosphere, are completely dark in their cores.
- 3. The source function of these lines should directly couple to the Planck function in the chromosphere and produce emission features (at least in their cores). Since this is not seen, Ayres has put forward the notion that the solar atmosphere has large amounts of cool (T < 4000 K) material at high altitudes due to a **bifurcation** in the plasma energy balance, induced by the strong surface emission of the  $\Delta v = 1$  bands themselves.
- 4. Ayres found a similar results for Arcturus and suggests that a stellar chromosphere actually only resides over a small fraction (< 20%) of a stellar (and solar) surface  $\Longrightarrow$  bifurcated atmospheres.
- 5. Meanwhile, Athay and Dere (1990, Astrophys. Journ., 358, 710) have tested the Ayres bifurcation idea through observations of the EUV emission lines of O I, C I, and Fe II. They found that the chromospheric temperature rise is present over 90% of the solar surface, in direct contradiction to Ayres' analysis of CO. Presently there is much research being carried out on this subject.

## K. Dynamical Modeling.

1. The Sun and many stars show evidence of dynamic processes in their atmospheres (*i.e.*, emission line variability, high mass-loss rates in some stars).

- 2. Mira-type variable stars are some of the most extreme cases of dynamical atmospheres, since they show evidence for strong, propagating shock waves in their atmospheres and have substantial mass loss ( $\dot{M} \gtrsim 10^{-7} M_{\odot}/\mathrm{yr}$ ). Bowen (1988, Astrophys. Journ., 329, 299) has modeled the atmospheres of these stars with a Lagrangian hydrodynamics code.
  - a) The time dependent calculations generally require many  $time\ steps\ (\sim 200)$ .
  - b) Many depth points or zones are required as well ( $\sim$ 500) to "converge" a model.
  - c) As such, the inclusion of radiative transfer into these types of problems are costly.
- 3. Although we will not get into the details of these types of calculations here, we will briefly mention them here. The Bowen code solves the coupled set of fluid equations to determine the atmospheric structure of pulsating stars. These fluid equations are nothing more than various conservation laws:
  - a) Conservation of momentum.
  - b) Conservation of mass.
  - c) Conservation of energy.
- 4. In these hydro-calculations, the pulsation of the star results in periodic shock structures which greatly extend the atmosphere with respect to HSE models, making semi-empirical models for these stars invalid. This produces a higher density in the outer atmosphere in these models, which in turn, makes dust formation more efficient. Radiation pressure on the dust then drives the strong stellar winds that are seen in these stars.